

**Accepted for publication in – Journal of Reinforced Plastics  
and Composites –**

**Published in July 19, 2013**

**DOI: DOI: 10.1177/0731684413497277**

EFFECTS OF FIBRE CONTENT AND TEXTILE STRUCTURE ON DYNAMIC-  
MECHANICAL AND SHAPE-MEMORY PROPERTIES OF ELO/FLAX  
BIOCOMPOSITES

**M. Fejős<sup>1</sup>, J. Karger-Kocsis<sup>1,2</sup> and S. Grishchuk<sup>3</sup>**

*<sup>1</sup>Department of Polymer Engineering, Faculty of Mechanical Engineering, Budapest  
University of Technology and Economics, H-1111 Budapest, Hungary*

*<sup>2</sup>MTA–BME Research Group for Composite Science and Technology, H-1111 Budapest,  
Hungary*

*<sup>3</sup>Institut für Verbundwerkstoffe GmbH, D-67663 Kaiserslautern, Germany*

**Corresponding author:**

Márta Fejős, Department of Polymer Engineering, Faculty of Mechanical Engineering,  
Budapest University of Technology and Economics, Műegyetem rkp. 3., Budapest H-  
1111, Hungary. Email: [mfejjos@gmail.com](mailto:mfejjos@gmail.com). Phone: +3614631525

**Submitted to Journal of Reinforced Plastics and Composites, May, 2013**

**Abstract**

Biocomposites were prepared using epoxidized linseed oil (ELO) and flax fibre reinforcements in different assemblies. ELO was cured by two different anhydrides to check how its thermomechanical properties can be influenced. As reinforcements nonwoven mat, twill weave and quasi-unidirectional textile fabrics with two different yarn finenesses were used. Their reinforcing effect was determined in **dynamic mechanical analysis (DMA)** in flexure. **DMA** served also to determine the glass transition temperature ( $T_g$ ). Shape memory properties were derived from quasi-unconstrained flexural tests performed near to the  $T_g$  of the ELO and its biocomposites. Flax reinforcement reduced the  $T_g$  that was attributed to off-stoichiometry owing to chemical reaction between the hydroxyl groups of flax and anhydride hardener. The shape memory parameters were moderate or low. They were affected by both textile content and type.

**Keywords**

shape memory polymer, biocomposite, flax reinforcement, epoxidized linseed oil, textile structure

## INTRODUCTION

Shape memory polymers (SMPs) are merging smart materials in different applications, especially in biomedical, aerospace and construction engineering fields. SMPs adopt reversibly a permanent or temporary shape under the combined action of mechanical load and external stimulus. The external stimulus is heat in most cases and the related SMPs are termed to thermally activated ones. The “switching” or transformation temperature, enabling the material to return to its permanent shape is the glass transition temperature ( $T_g$ ) for crosslinked systems. The permanent shape is guaranteed by the crosslinked network structure, whereas the temporary one results from its mechanical deformation above  $T_g$ . The macroscopic deformation applied is translated to conformational changes of the network and its constituents which are fixed (“frozen in”) by cooling the material whereby maintaining the shaping load. The strain energy, stored by this way, is released when the material is unloaded and heated above its  $T_g$ . This triggers conformational rearrangements of the molecular chains between the crosslinks via which the permanent shape is restored. A large body of works was already dealing with different SMPs and the related knowledge is well summarized in recent reviews.<sup>1,2,3,4</sup>

Preferred thermoset SMPs are epoxy (EP) resins based ones. EPs are selected owing to their favourable properties (heat and chemical resistance, high glassy and rubbery moduli, good adhesion to many substrates...) and versatility ( $T_g$  and modulus can be

easily tailored).<sup>5,6</sup> The development of shape memory (SM) EPs is hampered by their high glassy modulus and low ductility (elongation at break)<sup>5</sup> which are key parameters for biomedical applications which are now in the forefront of interest. This may change, however, profoundly by using epoxidized vegetable oils (EVOs) alone or as reactive diluents in traditional EPs. Cured EVOs show high ductility and low glassy and rubbery moduli. Moreover, blending EVO with traditional EP is a straightforward tool to tailor the thermomechanical properties, including  $T_g$ , of the related systems.<sup>7,8,9</sup> Last but not least, EVO is from renewable resources and thus their use is in line with the present public strategy, viz. “go green”. Attempts are even made to produce “bioresins” fully from renewable resources the properties of which are comparable to those of traditional “petroresins”.<sup>10</sup>

It is believed that SMPs can reach a broader utilization if their inherently low recovery force is enhanced. The latter requirement resulted in a vivid research activity with SMP composites (SMPCs). As reinforcements nano- and microparticles, traditional reinforcing fibres, also in different textile architectures, have been introduced. Among the man-made reinforcements textiles, composed of glass, carbon and aramid fibres, were mostly used.<sup>11</sup> By contrast, few works were dealing with biobased composites whose matrix and/or reinforcement derive from renewable resources. Natural fibre reinforcements are preferentially used in polymer composites nowadays. Albeit the stiffness and strength of natural fibres are inferior to those of man-made ones, their

ductility is markedly higher.<sup>12</sup> The high elongation at break of the fibres is of great relevance with respect to SM performance of the corresponding composites. High ductility is very beneficial for SMPCs enabling markedly higher deformations without failure than traditional reinforcing fibres. Moreover, at present natural fibres are available in other assemblies than non-wovens, mats and their effects on the SM performance was not yet topic of investigations.

Accordingly, this work was aimed at studying the type (non-woven, woven, quasi-unidirectional) and amount of flax fibre textiles on the SM properties of anhydride cured epoxidized linseed oil (ELO)-based biocomposites. The term “biocomposite” is justified by the fact that except of hardener and accelerator all other components are from renewable resources. Anhydride curing was reasoned by the fact that it works properly for EVOs by contrast to amine hardening.<sup>9,13</sup> In addition, the anhydride groups may react with the surface hydroxyl groups of flax creating a strong interphase which is the prerequisite of good quality composites.

## EXPERIMENTAL

Epoxidized linseed oil (ELO, Vikoflex 7190, Arkema, Blooming Prairie, MN, USA), which contains 9 wt% oxygen (epoxy equivalent: 89 g/equ), was hardened by two different anhydrides in order to see how the  $T_g$  of ELO can be influenced. ELO was hardened by a poly-hydroxylacid-anhydride (Epodur VP 675, Duroplast Chemie,

Neustadt/Wied, Germany), which has an anhydride equivalent of 158 g/equ, in stoichiometric ratio and in presence of 1 wt% tributyl amine (Merck Schuchardt OHG, Hohenbrunn, Germany). ELO was also hardened by methyltetrahydrophthalic anhydride (Aradur 917 CH, Huntsman Advanced Materials, Basel, Switzerland) in presence of 1.3 wt% 1-methylimidazole (Accelerator DY 070, also from Huntsman) again in stoichiometric ratio. These hardened ELOs, called ELO1 and ELO2, were produced in glass moulds<sup>14</sup> using a cure schedule of 2 hours at 100°C, 140°C and 180°C each. ELO2 was chosen as a matrix for the flax fibre-reinforced biocomposites.

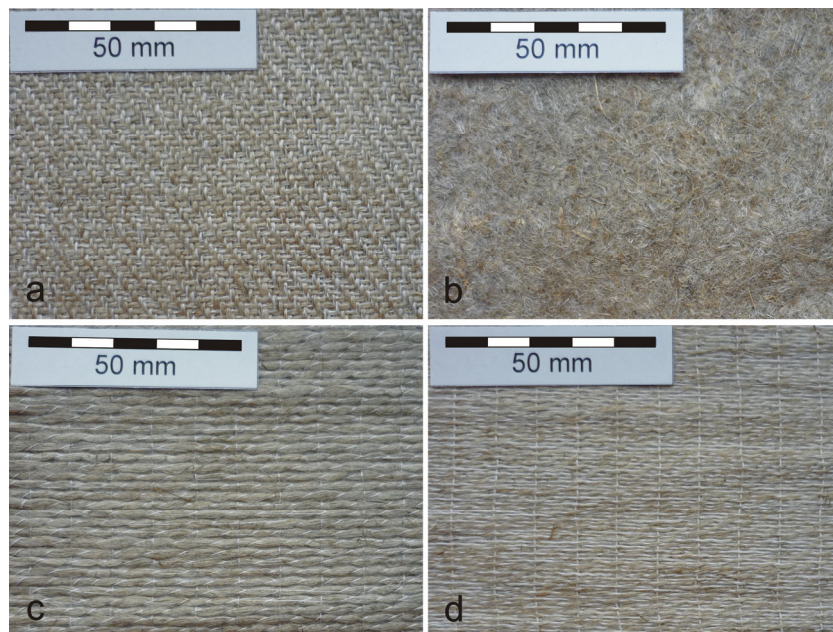


**Figure 1** Photographs of used flax fibre textiles: a) T b) NW c) UD420 d) UD275

The flax fibre fabrics were: twill (T, Figure 1a), quasi-unidirectional (UD) fabric composed of coarse yarns (UD420, Figure 1c), and fine yarns (UD275, Figure 1d), respectively, and flax fibre nonwoven mat (NW, Figure 1b) were purchased from Composites Evolution (Chesterfield, UK) and from J. Dittrich & Söhne Vliesstoffwerk GmbH (Ramstein-Miesenbach, Germany), respectively. Table 1 shows the area density and thickness data of the flax reinforcements. Nonwoven mat contains only flax fibres, but in case of woven fabrics flax fibres are twisted together with polyethylene-terephthalate (PET) fibre, whose amount was about 10 wt%, in order to strengthen natural fibres for processing. Because of natural fibres are able to adsorb water from air relatively fast (after 10 minutes reaches already more than 3 wt% at 21°C and 38% relative humidity), they were laminated in mould directly after taking out from oven, where were dried at 80°C for at least 4 hours.

Textile labelling	Textile structure	Nominal area density (g/m <sup>2</sup> )	Measured area density (g/m <sup>2</sup> )	Measured thickness (mm)
T	twill fabric	420	394	0.65±0,05
NW	nonwoven mat	220	238	0.63±0,11
UD420	quasi-UD fabric with coarse yarns	420	416	0.64±0,03
UD275	quasi-UD fabric with fine yarns	275	227	0.43±0,04

**Table 1** Properties of used flax fibre textiles

Composites were produced in a steel mould (Figure 2), which was sealed with room temperature vulcanizing silicone rubber (FAI Automotive plc, Bedfordshire, UK) and

sprayed with demoulding agent Indrosil 2000 (Indroma-Chemikalien, Bad Soden, Germany), using a Collin P300 P/M (Dr Collin GmbH, Ebersberg, Germany) hot press at 8 MPa pressure (loading rate:5.4 kPa/s). The cure program in the hot press was also 2-2 hours at 100°C, 140°C and 180°C, respectively. Thickness of product was adjusted for ca. 2 mm by the frame in the mould. Labelling, layer numbers and fibre content (determined by weighing) of produced biocomposites are tabulated in Table 2. All the samples were cut into 12 mm wide strip specimens. ELO1 and ELO2 samples were polished to get the same thickness as the biocomposite samples. Before measurements test specimens were conditioned at 70°C for 4 hours.

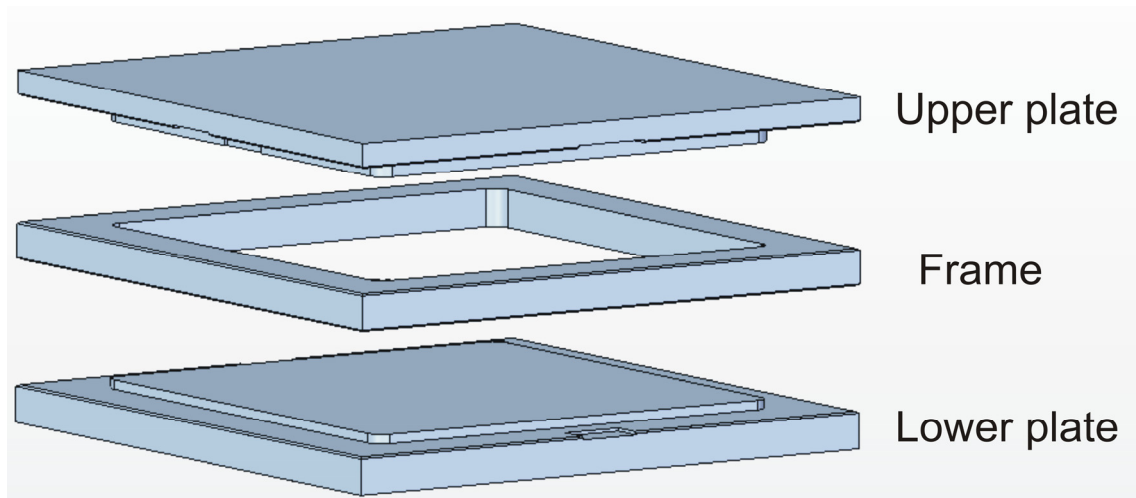


**Figure 2** Scheme of the used steel mould

Sample designation	Number of layers	Fibre content (wt%)
--------------------	------------------	---------------------



ELO2-T <sub>2</sub> (33)	2	33
ELO2-T <sub>3</sub> (47)	3	47
ELO2-T <sub>4</sub> (58)	4	58
ELO2-NW <sub>5</sub> (48)	5	48
ELO2-NW <sub>9</sub> (61)	9	61
ELO2-UD420 <sub>3</sub> (46)	3	46
ELO2-UD420 <sub>4</sub> (59)	4	59
ELO2-UD275 <sub>5</sub> (44)	5	44
ELO2-UD275 <sub>7</sub> (58)	7	58

**Table 2** Number of layers and fibre content of produced biocomposites. Note that the sample designation informs about the type of the flax fabric, its incorporated layers and amount in wt%

Dynamic mechanical analysis (DMA) was conducted on a DMA Q800 device (TA Instruments, New Castle, DE, USA) in 3-point bending arrangement with 50 mm span length. Heating rate, oscillation frequency and oscillation amplitude were 1°C/min, 1 Hz and 0.04%, respectively.

Though the DMA Q800 device can be used for shape memory test, its force limit (18 N) is too low for stiff samples like our biocomposites. Therefore we followed a quasi-unconstrained shape memory test on an Eplexor (GABO Qualimeter Testanlagen GmbH, Ahlden, Germany) machine which has a force limit of 150 N. However, the higher force limit has a disadvantage, namely higher minimum applicable force and lower precision in displacement measurement (1 nm for Q800 and 10 nm for GABO).

3-point bending tests with a span length of 40 mm were conducted on GABO Eplexor 150 N machine to examine the materials' deformability and determine the maximal strain ( $\epsilon_m$ ) for the shape memory test. For ELO2-UD420<sub>4</sub>(59) 3-point bending test was carried out at 100°C, 120°C and 150°C, respectively; while in other cases only at 100°C. This test was force controlled with loading rate of approximately 3 N/min. Dynamic load was set to the minimum, viz. 0.07 N, and the oscillation frequency selected was 5 Hz.

Quasi-unconstrained shape memory test was performed also on GABO Eplexor machine in the same arrangement as described above. At first samples were deformed to  $\epsilon_m=1\%$  at deformation temperature  $T_d=100^\circ\text{C}$ , than cooled to the storage temperature  $T_s=20^\circ\text{C}$  (except in case of ELO2-NW<sub>9</sub>(61), where  $T_s=0^\circ\text{C}$  was chosen), while  $\epsilon_m$  was kept constant. After unloading, the bent specimens were heated up to a temperature higher than  $T_g$  ( $T_h=140^\circ\text{C}$ ) with  $3^\circ\text{C}/\text{min}$  heating rate, while a contact force of  $0.5\pm 0.35$  N was maintained.

## RESULTS AND DISCUSSION

### DMA

Test results are usually reported by showing the storage modulus ( $E'$ , MPa), loss factor ( $\tan\delta$ , -) and loss modulus ( $E''$ , MPa) as a function of the temperature ( $T$ , °C).  $T_g$  values were derived from all of the above DMA traces – CF. Table 3.  $T_g^{E'}$  is the onset point of

$E'(T)$  curve,  $T_g^{tan\delta}$  and  $T_g^{E''}$  are peak temperatures of  $tan\delta(T)$  and  $E''(T)$  curves, respectively. The storage modulus is a good indicator for the reinforcing effect achieved through different textile types and amounts, provided that the measurements were performed with strictly the same test parameters. DMA curves of the ELO samples (Figures 3 and 4) show that  $T_g$  of the cured ELO can be varied, in fact, by using different anhydrides for hardening. For preparation of the flax fabric-reinforced biocomposites ELO2 was chosen as matrix because of its higher  $T_g$ .

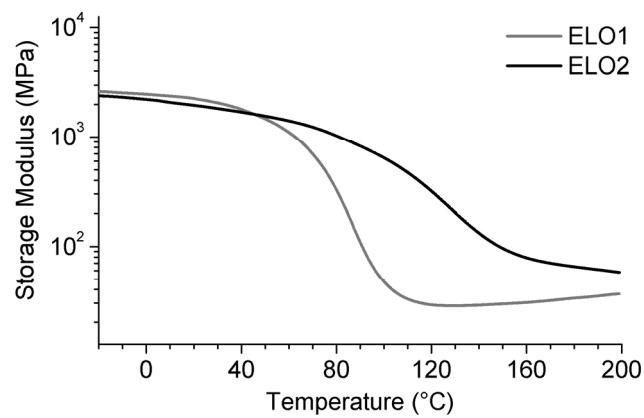


**Figure 3**  $E'(T)$  curves of reference samples (ELO1 and ELO2)

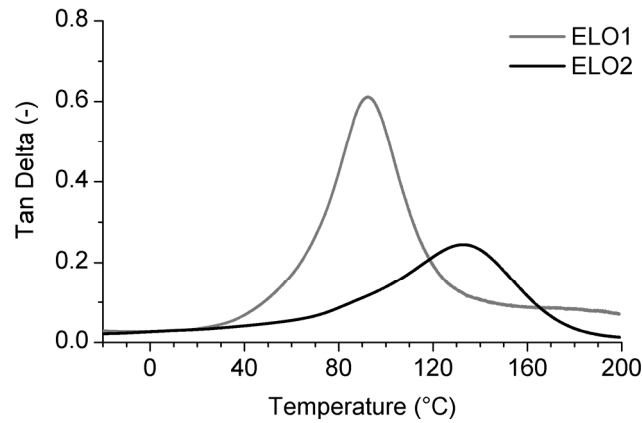


**Figure 4**  $Tan\delta(T)$  curves of the reference samples (ELO1 and ELO2)

$E'(T)$  traces of the biocomposites reinforced with twill flax fabric in different amount are depicted in Figure 5. In line with the expectation with increasing fibre content  $E'$  increases in both the glassy and rubbery states. On the other hand,  $T_g$  decreased with increasing fibre content (Figure 6). This is probably an effect of the anhydride hardener which is reacting with the surface hydroxyl groups of flax. As a consequence, the initial stoichiometry is blurred; the outcome is  $T_g$  reduction, which correlates with Boquillon's<sup>15</sup> results.

Comparing the  $E'(T)$  traces of the biocomposites with different textile structures at similar fibre content, one can resolve that reinforcing efficiency in the glassy state is: UD420>UD275>T>NW. NW strengthens the ELO2 matrix better in rubbery state than T fabric because of the PET fibre content. For shape memory composite incorporation of twill fabric seems to be the right choice, because the ratio of the glassy to rubbery

modulus is higher<sup>16</sup> compared to the nonwoven mat. Results of the DMA tests, viz.  $T_g$  data according to different determinations, glassy and rubbery moduli at various temperatures, are collected in Table 3.

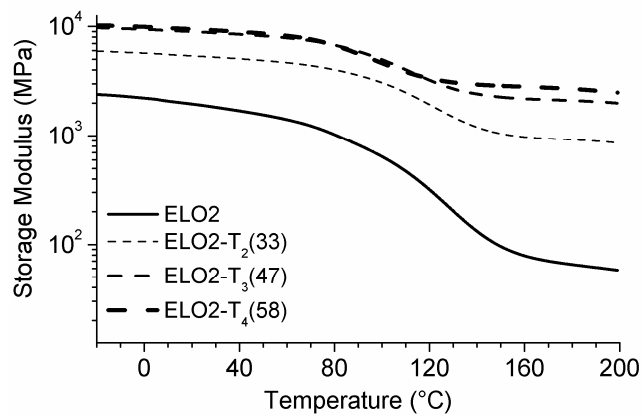


**Figure 5**  $E'(T)$  curves of reference sample (ELO2) and biocomposites with different fibre content

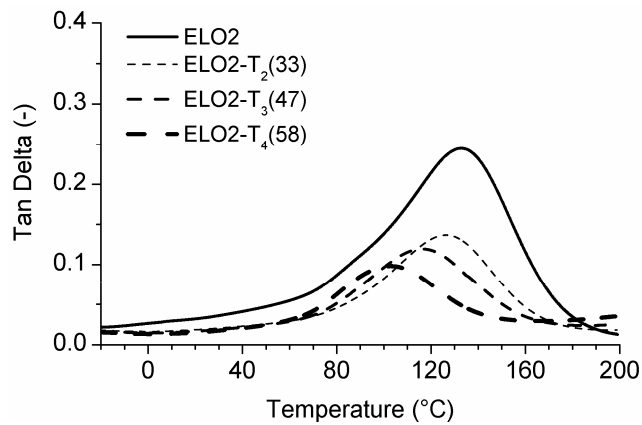


**Figure 6**  $Tan\delta(T)$  curves of reference sample (ELO2) and biocomposites with different fibre content

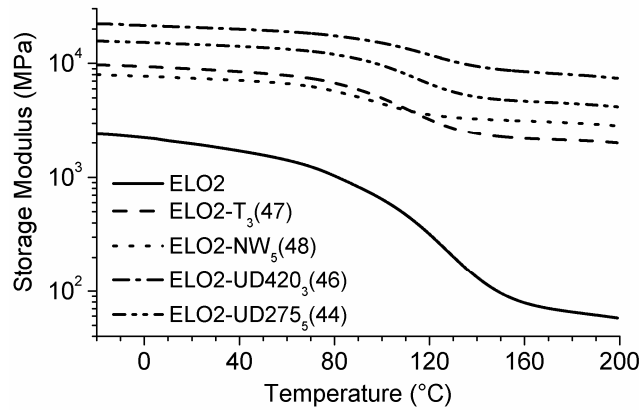


**Figure 7**  $E'(T)$  curves of the reference sample (ELO2) and related biocomposites with different textile structure. Note that the flax content of the biocomposites is comparable (44-48 wt%)

Samples	$T_g^{E'}$ (°C)	$T_g^{tan\delta}$ (°C)	$T_g^{E''}$ (°C)	$E'_{20^\circ C}$ (MPa)	$E'_{100^\circ C}$ (MPa)	$E'_{150^\circ C}$ (MPa)
ELO1	64	93	65	2270	48	29
ELO2	85	133	89	1960	646	96
ELO2- $T_2(33)$	86	126	111	5390	3080	1050
ELO2- $T_3(47)$	78	116	103	8970	4990	2270
ELO2- $T_4(58)$	67	103	92	9450	4640	2880
ELO2-NW $_5(48)$	67	103	96	7430	4470	3210
ELO2-NW $_9(61)$	54	79	74	10040	4894	4360
ELO2-UD420 $_3(46)$	90	124	116	20630	15090	8840
ELO2-UD420 $_4(59)$	67	95	90	25850	15090	11610
ELO2-UD275 $_5(44)$	84	118	110	14680	9640	4840

ELO2-UD275<sub>7</sub>(58)      75                  109                  103                  23750                  16460                  11470

**Table 3** Glass transition temperatures and storage moduli at different temperatures read from DMA measurements. (Note: data derived from two parallel tests)

### 3-point Bending Test

Above  $T_g$  (at 120 and 150°C) the flexibility of the stiffest biocomposite specimen is very low (Figure 8), 1% strain cannot be reached without failure of the material. Therefore for shaping a deformation temperature ( $T_d$ ) of 100°C was selected for all the samples. Recall that this  $T_d$  is very close to the actual  $T_g$  (cf. Table 3). According to the literature shape memory effect can be triggered also when  $T_d$  is set near or even under  $T_g$ .<sup>17</sup>

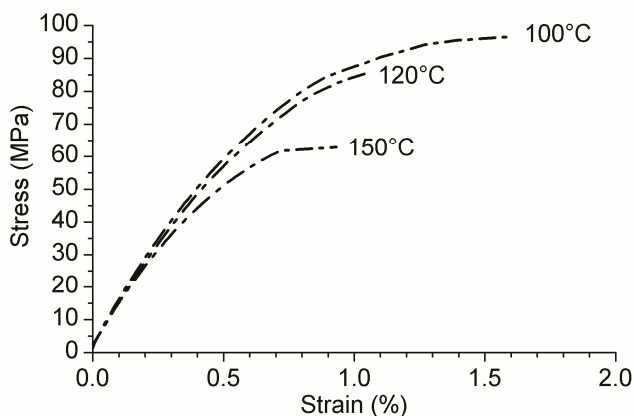


**Figure 8** Flexural stress-strain curves of ELO2-UD420<sub>4</sub>(59) at different temperatures

Before shape memory tests the samples were bent at  $T_d$  until break. This test served to determine the maximum deformation strain ( $\varepsilon_m$ ) which does not cause substantial damage and thus well applicable for shape memory programming. Based on the stress-strain curves, registered at  $T=100\text{ }^\circ\text{C}$  (Figure 9 and 10),  $\varepsilon_m = 1\%$  has been selected.

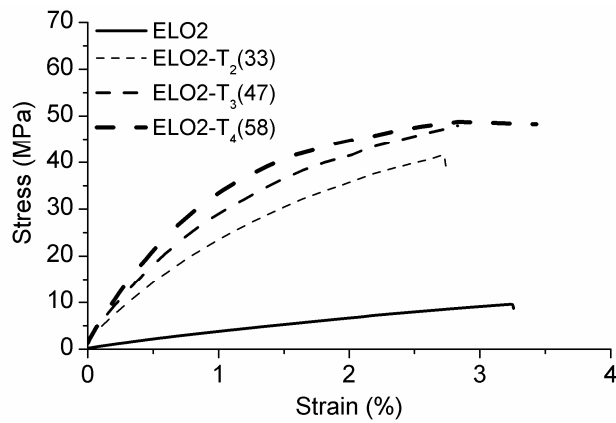


**Figure 9** Flexural stress-strain curves of ELO2 and related twill weave-reinforced biocomposites with different flax fibre contents at  $100\text{ }^\circ\text{C}$

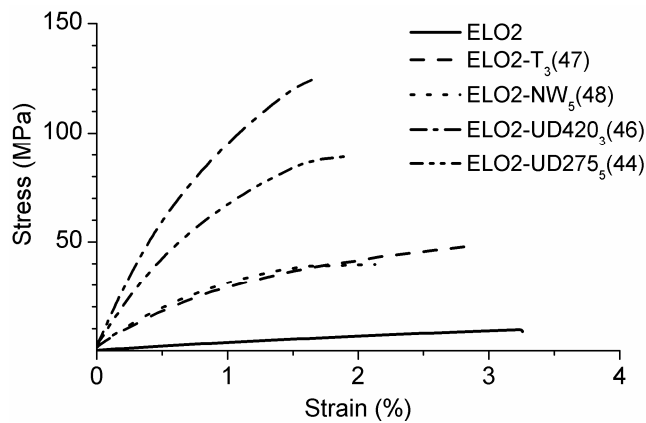




**Figure 10** Flexural stress-strain curves of ELO2 and related biocomposites with different textile structures with comparable flax contents at 100°C

### Shape Memory Behaviour

Shape memory performance is characterised in this work by the loading stress ( $\sigma_{load}$ ), which is the highest stress measured during deforming the specimen to  $\varepsilon_m$  and which is in close relation to recovery stress;<sup>18</sup> shape fixity ratio ( $R_f$ , %, Equation 1), where  $\varepsilon_u$  is the strain measured after unloading at  $T_s$ ; shape recovery ratio ( $R_r$ , %, Equation 2), where  $\varepsilon_p$  is the strain measured after recovery at  $T_h$  and  $\varepsilon_0$  is the initial strain (in our case it is always zero); and combined shape memory ratio ( $R_\Sigma$ , %, Equation 3), which is equal to  $R_f(100-R_r)$ , if  $\varepsilon_0$  is zero.

$$R_f = \frac{\varepsilon_u}{\varepsilon_m} \cdot 100 \quad (1)$$

$$R_r = \frac{\varepsilon_m - \varepsilon_p}{\varepsilon_m - \varepsilon_0} \cdot 100 \quad (2)$$

$$R_\Sigma = \frac{\varepsilon_u - \varepsilon_p}{\varepsilon_m - \varepsilon_0} \cdot 100 \quad (3)$$

Table 4 lists the shape memory properties of the samples. ELO2 has shape recovery ratio of 25%, which is very low. This is because the material is much too weak above  $T_g$  to move against the contact force.  $R_\Sigma$  increases with increasing fibre content in case of

twill flax fabric reinforcement. Its value does not change for NW, and decreases for both UD flax fabric reinforcements.

Samples	$\sigma_{load}$ (MPa)	$R_f$ (%)	$R_r$ (%)	$R_\Sigma$ (%)
ELO2	4	92	25	17
ELO2-T <sub>2</sub> (33)	23	70	64	33
ELO2-T <sub>3</sub> (47)	35	70	75	45
ELO2-T <sub>4</sub> (58)	29	78	72	50
ELO2-NW <sub>5</sub> (48)	30	67	76	43
ELO2-NW <sub>9</sub> (61)	27	77	66	43
ELO2-UD420 <sub>3</sub> (46)	93	54	75	28
ELO2-UD420 <sub>4</sub> (59)	95	42	77	19
ELO2-UD275 <sub>5</sub> (44)	65	65	76	41
ELO2-UD275 <sub>7</sub> (58)	79	61	76	37

**Table 4** Shape memory properties of ELO2 and related flax fabric reinforced biocomposites. (Note: data achieved on a single specimen)

As expected based on our previous study<sup>14</sup> continuous fibre reinforcement lowered  $R_f$ , but this reduction could be moderated by choosing suitable textile structures. As it can be seen in Figure 11  $R_f$  decreases the less in for the twill fabric.  $R_r$  is similar for all the biocomposites. Figure 11 illustrates also the reported strain values and from those calculated ratios. In the temperature range of 20-40°C the strain increases slightly. This is supposed to be an effect of the instrument. Therefore in present case  $\varepsilon_u$  was defined as the maximum of strain during reheating before shape recovery starts.

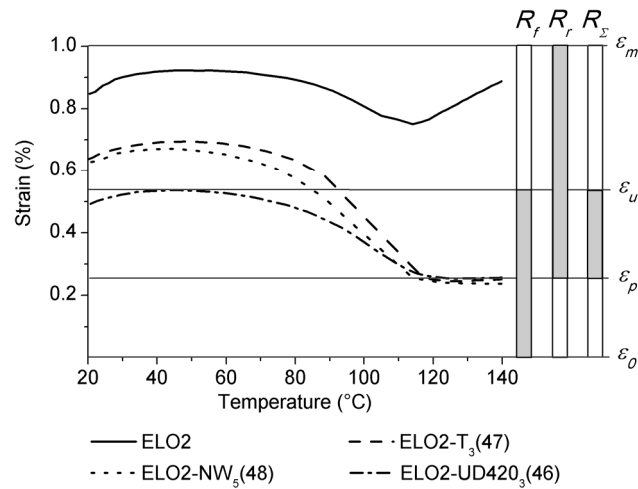


**Figure 11** Shape recovery of ELO2 and its biocomposites with different textile structures. Reported strain values and ratios are marked for the sample ELO2-UD420<sub>3</sub>(46)

Decrease of  $R_f$  can be also controlled by choosing a textile containing fine yarns. The effect of yarn thickness is depicted in a 3D representation of the shape memory cycle (Figure 12). This figure also shows the difference between the quasi-UD reinforced biocomposites and reference ELO2. Note that the loading stress ( $\sigma_{load}$ ) of the composites is much higher than that of neat matrix. This is achieved, however, at cost of the shape fixity, which decreased.

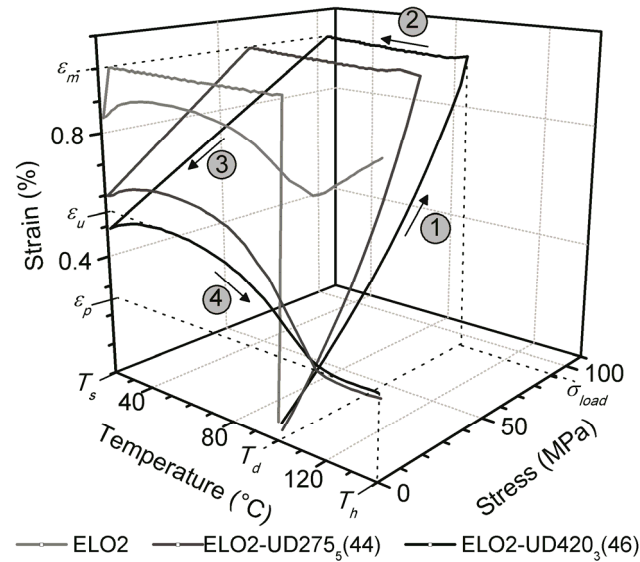


**Figure 12** 3D representation of shape memory behaviour of the reference sample (ELO2) and its UD-reinforced biocomposites with different yarn thickness. In case of ELO2-UD420<sub>3</sub>(46) the numbers in circles indicate the steps of shape memory test: 1) deforming at  $T_d=100^{\circ}\text{C}$  to  $\varepsilon_m=1\%$ , 2) shape fixing when cooling to  $T_s=20^{\circ}\text{C}$  while keeping  $\varepsilon_m=1\%$ , 3) unloading, 4) shape recovery under  $0.5\pm 0.35$  N contact force

## CONCLUSION

Based on this work devoted to study the effects of the amount and types of various flax fibre textiles on the dynamic mechanical and shape memory properties of biocomposites with anhydride cured epoxidized linseed oil (ELO) matrix, the following conclusions can be derived:

- Properties of the cured ELO can be tailored by the anhydride type.

- Flax reinforcement reduced the  $T_g$  of ELO which can be traced to the chemical reaction between the surface hydroxyl groups of flax and anhydride hardener associated with stoichiometry offset. The flexural reinforcing effect of the flax fabrics based on the course of the glassy storage modulus as a function of temperature followed the ranking: nonwoven < twill weave < quasi-unidirectional (UD). UD fabric composed of thick yarns performed better than that of thin ones.
- The shape memory properties derived from flexural tests were low or moderate. This was due to the fact that  $T_g$  was selected as deformation temperature ( $T_d$ ) in the related tests. This was compensated, however, with considerable recovery stresses reaching almost 100 MPa for the biocomposite containing at about 60 wt% UD fabric with thick yarns. The shape memory characteristics changed more with the type of flax reinforcement than with its amount.

### **Funding**

This work was supported by the Hungarian Research Fund [OTKA NK 83421]; the European Union's Seventh Framework Programme [Clean Sky Joint Technology Initiative No° 298090]; and by the Hungarian National Development Agency [TÁMOP-4.2.1/B-09/1/KMR-2010-0002, TÁMOP-4.2.2/B-10/1-2010-0009, TÁMOP-4.2.2.A-11/1/KONV-2012-0036].

## References

1. Behl M and Lendlein A. Actively moving polymers. *Soft Matter* 2007; 3: 58–67.
2. Mather PT, Luo XF and Rousseau IA. Shape memory polymer research. *Annual Review of Materials Research* 2009; 39: 445–471.
3. Xie T. Recent advances in polymer shape memory. *Polymer* 2011; 52: 4985–5000.
4. Hu J, Zhu Y, Huang H, Lu J. Recent advances in shape-memory polymers: Structure, mechanism, functionality, modeling and applications. *Progress in Polymer Science* 2012; 37: 1720–1763.
5. Rousseau IA and Xie T. Shape memory epoxy: Composition, structure, properties and shape memory performances. *J Mater Chem* 2010; 20: 3431–3441.
6. Kumar KSS, Biju R and Nair CPR. Progress in shape memory epoxy resins. *Reactive and Functional Polymers* 2013; 73: 421–430.
7. Tan SG and Chow WS. Biobased epoxidized vegetable oils and its greener epoxy blends: A review. *Polymer-Plastics Technology and Engineering* 2010; 49: 1581–1590.
8. Wang R and Schuman TP. Vegetable oil-derived epoxy monomers and polymer blends: A comparative study with review. *Express Polym Lett* 2013; 7: 272–292.

9. Karger-Kocsis J, Grishchuk S and Soroachynska L. Curing, gelling thermomechanical and thermal decomposition behaviors of anhydride-cured epoxy (DGEBA)/epoxidized soybean oil (ESO) compositions. *Polym Eng Sci*, In Press.
10. Liu XQ, Huang W, Jiang YH, et al. Preparation of a bio-based epoxy with comparable properties to those of petroleum-based counterparts. *Express Polym Lett* 2012; 6: 293–298.
11. Meng H and Li G. A review of stimuli-responsive shape memory polymer composites. *Polymer* 2013; 54: 2199–2221.
12. Mohanty AK, Misra M. and Hinrichsen G. Biofibres, biodegradable polymers and biocomposites: An overview. *Macromol Mater Eng* 2000; 276/277: 1-24.
13. Tan SG and Chow WS. Thermal properties, curing characteristics and water absorption of soybean oil-based thermoset. *Express Polym Lett* 2011; 5: 480–492.
14. Fejős M, Romhány G and Karger-Kocsis J. Shape memory characteristics of woven glass fibre fabric reinforced epoxy composite in flexure. *J Reinf Plast Compos* 2012; 31: 1532–1537.
15. Boquillon N. Use of an epoxidized oil-based resin as a matrix in vegetable fibers-reinforced composites. *J Appl Polym Sci* 2006; 101: 4037–4043.

16. Ratna D and Karger-Kocsis J. Recent advances in shape memory polymers and composites: A review. *J Mater Sci* 2008; 43: 254–269.
17. Feldkamp DM and Rousseau IA. Effect of the deformation temperature on the shape-memory behavior of epoxy networks. *Macromol Mater Eng* 2010; 295: 726–734.
18. Fejős M and Karger-Kocsis J. Shape memory performance of asymmetrically reinforced epoxy/carbon fibre fabric composites in flexure. *Express Polym Lett* 2013; 7: 528–534.